Pediatric Neurosurgery

Research Article

Pediatr Neurosurg 2023;58:383–391
DOI: 10.1159/000533168

Received: December 20, 2022
Accepted: May 2, 2023
Published online: September 13, 2023

A New Measure of Posterior Morphology in Sagittal Craniosynostosis: The Occipital Bullet Index

Griffin P. Bins Deborah Cull Ryan G. Layton Samuel Kogan Larry Zhou
Blake Dunson Lisa R. David Christopher M. Runyan

Department of Plastic and Reconstructive Surgery, Wake Forest Baptist Medical Center Winston Salem, NC, USA

Keywords
Craniosynostosis · Sagittal · Scaphocephaly · Occipital bullet · Morphology · 3D photography

Abstract
Introduction: Sagittal craniosynostosis (SC) is associated with scaphocephaly, an elongated narrow head shape. Assessment of regional severity in the scaphocephalic head is limited by the use of serial computed tomographic (CT) imaging or complex computer programing. Three-dimensional measurements of cranial surface morphology provide a radiation-free alternative for assessing cranial shape. This study describes the creation of an occipital bulleting index (OBI), a novel tool using surface morphology to assess the regional severity in patients with SC. ***Methods:*** Surface imaging from CT scans or 3D photographs of 360 individuals with SC and 221 normocephalic individuals were compared to identify differences in morphology. Cartesian grids were created on each individual's surface mesh using equidistant axial and sagittal planes. Area under the curve (AUC) analyses were performed to identify trends in regional morphology and create measures capturing population differences. ***Results:*** The largest differences were located in the medial regions posteriorly. Using these population trends, a measure was created to maximize AUC. The OBI has an AUC of 0.72 with a sensitivity of 74% and a specificity of 61%. When the frontal bossing index is applied in tandem, the two have a sensitivity of 94.7% and a specificity of 93.1%. Correlation between the two scores in individuals with SC was found to be negligible with an intraclass correlation coefficient of 0.018. Severity was found to be independent of age under 24 months, sex, and imaging modality. ***Conclusions:*** This index creates a tool for differentiating control head shapes from those with SC and has the potential to allow for objective evaluation of the regional severity, outcomes of different surgical techniques, and tracking shape changes in individuals over time, without the need for radiation.

Introduction

Premature sagittal suture fusion impairs biparietal expansion of the skull, resulting in anterior and posterior skull elongation, termed frontal bossing and occipital bulleting [1]. The frontal and posterior elongation of sagittal craniosynostosis (SC) may be accompanied by other more minor morphologic characteristics [1]. Many surgical interventions are employed to treat these morphologic anomalies: sagittal suturectomy with helmeting

karger@karger.com
www.karger.com/pne

Correspondence to:
Christopher M. Runyan, crunyan@wakehealth.edu

or spring-assisted expansion, or cranial vault remodeling involving the anterior 2/3rds, posterior 2/3rds, central or total calvarium. However, it is unclear whether any technique is superior for correcting these deformities or if the patient's growth pattern should influence choice of intervention. Consensus is limited by a lack of measures evaluating regional cranial morphology and the resulting lack of postoperative outcomes data.

Multiple attempts have been made to quantify frontal bossing [2–7]. However, few attempts have been made to quantify the posterior prominence despite literature indicating the high frequency of individuals with SC developing a posterior prominence [8, 9].

Posterior cranial shape evaluation in patients with SC has been volumetric [10–12] or dependent upon computed tomographic (CT)-based measures [13, 14]. However, noninvasive surface laser- or 3D photographic modalities have been used to create 3D surface models without the use of radiation [15], providing a safe option for tracking growth in a pediatric population allowing for serial pre- and postoperative evaluation. A tool utilizing surface point analysis would allow for inexpensive and radiation-free data acquisition to better understand the effect of different operative interventions. The purpose of this study was to generate a tool for objective quantification of the posterior prominence observed in SC patients. We hypothesize that using surface imaging modalities we can define an objective measure to identify morphologic differences in the posterior cranium of individuals with SC.

Methods

Database Creation

The method for obtaining preoperative and control population scans was previously described [16] but is summarized as follows. Cranial and craniofacial CT scans and 3D stereophotograms of normocephalic patients were obtained with even age and sex distribution (0–72 months) for characterization of normal head shape. CT scans of patients with SC were acquired from the Wake Forest Craniofacial Imaging Database for analysis of surface anatomy. CT scans were excluded if the following occurred: missing landmarks or missing cranial soft tissue, low resolution, misaligned CT slices, or medical device interference.

CT scans were thresholded creating a hairless model of the skin surface. CTs and 3D photos were exported as stereolithographic files and landmarked at the sellion and bilateral tragions. Models were then reoriented with the origin defined as the intersection of the line that intersects both tragions, and the perpendicular line intersecting the sellion. The axes were set with the x-axis right to left, the z-axis dorsal to ventral, and the y-axis caudal to cephalad.

Three sets of planes were created for each 3D stereolithographic file: the axial planes at the intersection of the x- and z-axes (Fig. 1a), the sagittal planes at the intersection of the y- and z-axes (Fig. 1b), and the coronal planes at the intersection of the x- and y-axes (Fig. 1c). The mid-coronal plane was positioned perpendicular to the axial plane and passing through the bilateral tragion. Ten equidistant axial, sagittal, and coronal planes were created from the origin based on the cranial height (axial), width (sagittal), and length (coronal).

Curves were created along the intersections of the generated planes and the surface of the 3D models, termed the axial and sagittal curves. The overlay of the axial and sagittal curves created a Cartesian grid (Fig. 2), and the intersecting points (vertices) were exported as 3D coordinates.

Population Analysis

In order to control for variation in head size, we examined multiple parameters to identify those least affected by diagnosis. Parameters examined (Table 1) for all control and SC patients included projection of the sellion relative to the mid-coronal plane, head circumference at multiple axial levels, width at the widest (4th) axial level, height from the origin to the intersection of the mid-coronal and mid-sagittal plane, and total cranial length at the longest (4th) axial level. The parameter with the least interaction relative to diagnosis (projection of the sellion) was utilized to normalize for growth when analyzing the vertices along the posterior surface grid. Occipital protrusion was then defined as the distance of an individual axial/sagittal vertex along the posterior grid to the mid-coronal plane, divided by the sellion projection for the same patient. After identifying the most distinct points, targeted measures were created using groupings of unique points. Each individual and grouped measure was ultimately assessed using the receiver operating characteristic (ROC) curve combined with area under the curve analysis to identify the tool that generated the most distinct metric for describing occipital protrusion, the occipital bullet index (OBI).

The tools created with these controls were then analyzed with regard to area under the ROC curve and correlation to clinician scoring. After determining the most effective tool, outliers and potential confounding variables were analyzed.

R Statistical Software (version 4.1.0; R Foundation for Statistical Computing, Vienna, Austria) was used for all other statistical calculations, $\alpha = 0.05$. Descriptive statistics were calculated using means ± SD or percentages and Shapiro-Wilk, Wilcoxon Rank-Sum test, and F tests were used to confirm normality and homogeneity of variances. The Pearson's Product Correlation was calculated to test for independence between ratios and age. The Welch two sample t test or independent t test was also employed to confirm independence between ratios, sex, and imaging modality. Results indicated no significant correlation between any of these variables.

Validation

Two craniofacial surgeons were given identical AP, lateral, and superior views of the posterior hemispheres of 28 3D surface models from patients with sagittal CS for independent assessment of dysmorphology in the occipital region. The models were placed in order from most to least severe, and then reviewed and revised, scoring individuals from 1 to 10, with 10 indicating most severe protrusion. The scores were evaluated using a Cohen's kappa to assess inter-rater reliability. Average clinician score was then assessed for correlation to the OBI.

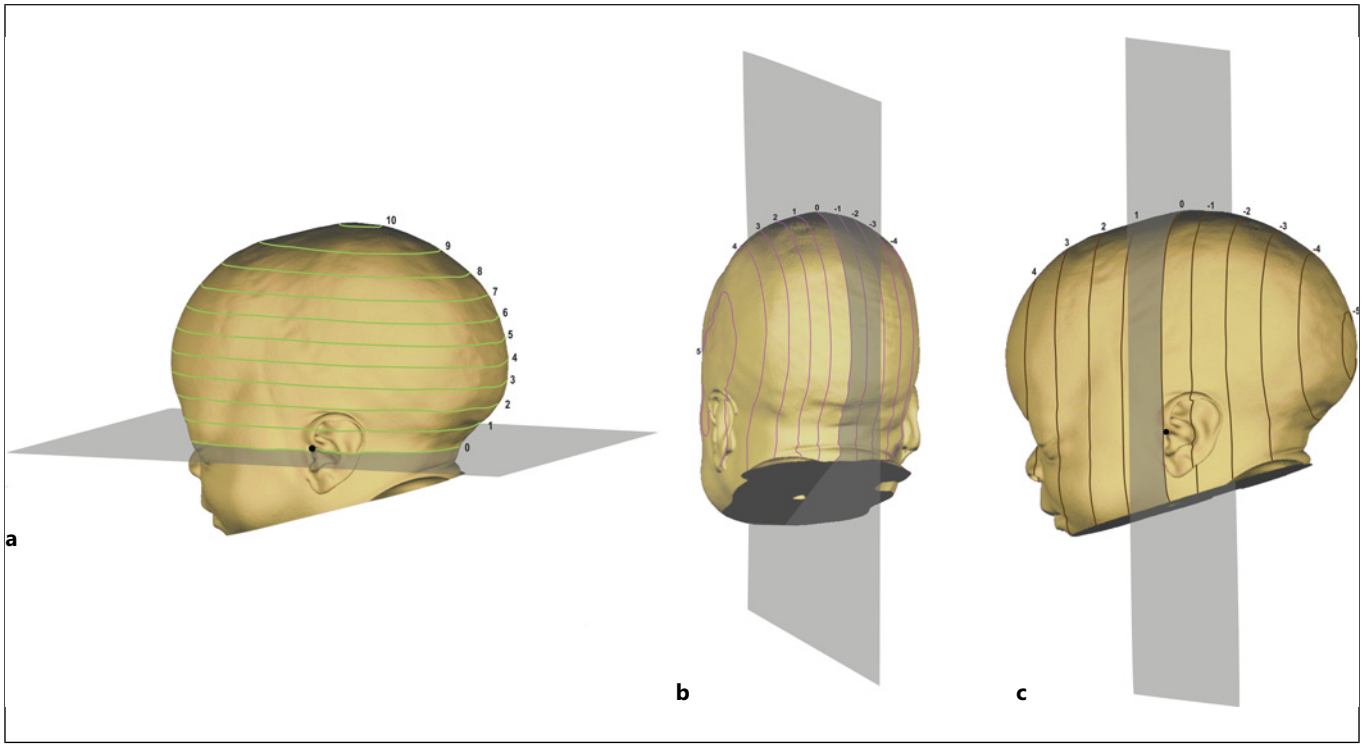

Fig. 1. a–c Generation of axial, sagittal, and coronal plane systems. **a** Creation of baseline axial plane using the sellion and tragions to define axial plane 0 (A0). Ten equidistant planes were created from A0 using the height at the mid-coronal plane, with the most cephalic plane designated A10. **b** The mid-sagittal plane (S0) was defined as the plane perpendicular to the baseline axial plane while passing through the sellion and origin. Five equidistant sagittal planes were created on both the right side (+5) and the left side (−5) of S0. **c** The mid-coronal plane (C0) was created perpendicular A0 through the bilateral tragions. Five equidistant coronal planes were created both anterior (+5) and posterior (−5) to C0. The para-sagittal and para-coronal plane spacing were determined using the head width and length at axial plane 4.

Results

Scan Selection

Of the 416 SC and 1,512 control CT scans and 3D-photographs identified, 360 SC and 221 control individuals remained after exclusion criteria were applied. Control CT scans were composed of normocephalic pediatric patients seen in the Emergency Department without fractures or soft tissue damage. The study group was comprised of patients evaluated for SC seen by the Plastic Surgery Department which routinely orders high-resolution CT scans. Thus, a lower percentage needed to be removed due to low scan resolution.

Population Analysis

All surface points formed by the posterior intersection of the axial and sagittal planes were analyzed in the normal and SC populations to identify differences. The ratios describing protrusion and population averages at each point are depicted in Figure 3. The point of maximal posterior protrusion was (S0, A4) in both the SC and control populations. The percent difference between the two populations increased at central and inferior points and peaked at the intersection of axial plane 2 and sagittal plane 0 (S0, A2).

Tool Creation

To control for head size variation, we evaluated different denominators for normalization, including the projection of the sellion, circumference, width, height, and total cranial length. The metric least affected by diagnosis was found to be the sellion projection (Table 1).

Point (S0, A2) had the greatest individual area under the ROC curve (AUC) with a value of 0.7619. The AUC calculated using midline points yielded similar results from levels A1 to A5, with all having an AUC greater than 0.7207. The correlation coefficient (CC) when comparing point projection and clinician evaluation ranged from 0.18 (S0, A2) to a maximum of 0.49 (S0, A7). The ratio of projection of point (S0, A5) to the projection of the sellion

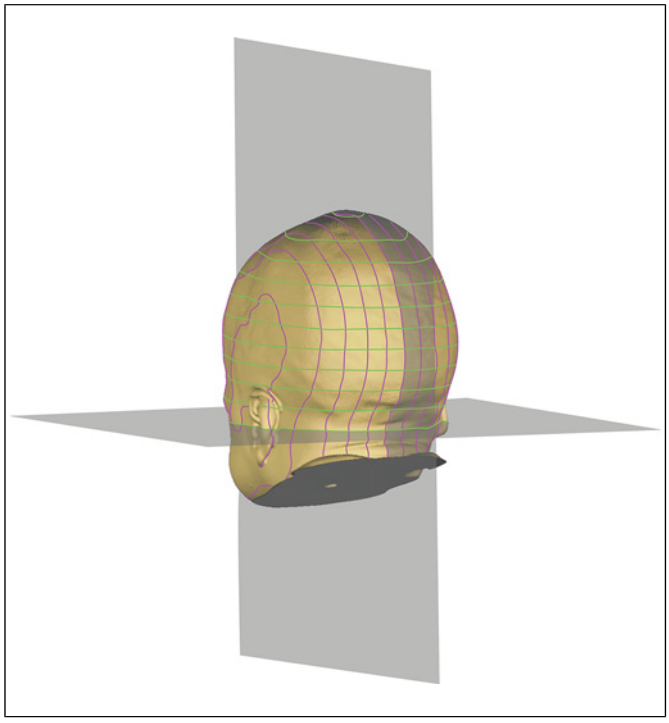

Fig. 2. Overlay of axial and sagittal plane systems. A Cartesian grid created using the axial and sagittal planes (AS grid) contains points of intersection (vertices) on the posterior surface of the scalp. These points can be described as a coordinate (x, y, z). Within the AS grid, a change in the x and y directions occur at discrete intervals specific to the respective axial or sagittal plane of interest. The z value is continuous and describes the posterior surface projection found at a specific intersection of an axial and sagittal plane.

had the largest combination of AUC (0.7207) and CC (0.469) and was used to create the OBI with a sensitivity of 0.742 and a specificity of 0.610 at a cutoff of 1.069 (Fig. 4, 5).

Analysis for Potential Confounding Variables:

Individual outliers were reviewed during initial analysis. All scores were validated except the highest-scoring control patient. Upon review of this patient's CT scan, a completely fused sagittal suture was identified and this patient was subsequently removed from the final analysis. Two raters landmarked the same 24 masks to determine inter-rater reliability. The inter-rater CC was calculated to be 0.97. The results of Pearson's product-moment correlation determined that the correlation between age (months) and the OBI ratio in the control group was not significantly different from zero ($p = 0.725$). Similarly, the Spearman's rank correlation showed that age and OBI ratio are independent in the SC patient sample ($p = 0.4595$). A Welch two sample t test demonstrated biologic sex was not correlated with the OBI ratio in the control group ($p = 0.6854$) or the SC group ($p = 0.881$). Finally, the use of two imaging modalities (CT and 3DMD) in the control group did not have a significant effect on the OBI ($p = 0.1296$). Together these indicate that the OBI is independent of age (within the examined range), sex, and diagnosis.

Discussion

The morphology of SC is well established and perhaps best demonstrated by both anterior and posterior prominences. Previous study indicates a posterior bullet is more common than anterior bossing [8, 9]. Despite a well-established morphology, patient evaluation remains subjective, and limited objective measurements focus on the anterior cranium. Objective measures are needed as clinician visual assessment of global and regional severity varies considerably [17–21]. This inconsistency coupled with the absence of a tool targeting posterior anatomy limits surgeon ability to objectively discuss operative results and evaluate longevity of surgical correction. For these reasons, tools are needed to quantify and standardize regional morphology to aid in preoperative planning and evaluation of short and long-term outcomes [6].

Posterior cranial analysis has been largely limited to volumetric study [10–12]. While volume is a 3D measure, it lacks dimensional specification. For example, an increase in protrusion coupled with decrease in width yields minimal volumetric change. Vu et al. [10] hypothesized that the posteroinferior expansion observed in patients with SC is not sufficient to compensate for transverse constriction. As a result, posterior volumetric differences have been statistically insignificant [10–12]. We therefore posit that volume-based measure may be insufficient for characterizing the atypia of the posterior cranium in this population.

The cephalic index (CI) is a two-dimensional direct anthropomorphic measure of the ratio of maximum cranial width (euryon-euryon) to maximum length (anterior-posterior or glabella-opisthocranion) developed in the 1,800s for skull osteology [22] and is widely used but also criticized for its shortcomings [6, 13, 23]. The CI may not correlate with clinical severity [4] and is unable to provide a regionalized (frontal vs. occipital predominance) and comprehensive three-dimensional measure of the scaphocephalic cranium.

Table 1. Influence of sagittal craniosynostosis on head surface parameters

Variable	% of variable due to diagnosis	Confidence interval, %
Height[1] at intersection of sagittal and coronal plane 0	−3.6	−5.0, −2.2
Length at axial plane 4 and sagittal plane 0	10.1	8.9, 11.4
Width at axial plane 4 and coronal plane 0	−7.1	−8.6, −5.6
Circumference at axial 1	6.9	4.9, 8.9
Circumference at axial 2	7.0	5.3, 8.7
Circumference at axial 3	4.5	3.3, 5.7
Circumference at axial 4	4.5	3.4, 5.7
Circumference at axial 5	4.3	3.2, 5.5
Circumference at axial 6	4.0	2.8, 5.3
Circumference at axial 7	3.3	2.1, 4.6
Circumference at axial 8	4.1	2.6, 5.5
Circumference at axial 9	6.6	4.7, 8.6
Circumference at axial 10	5.3	−7.3, 17.9
Sellion protrusion	3.8	1.9, 5.6
(S+/−3, A5) average protrusion	16.6	14.4, 18.7

[1]Height calculated relative to axial plane 0.

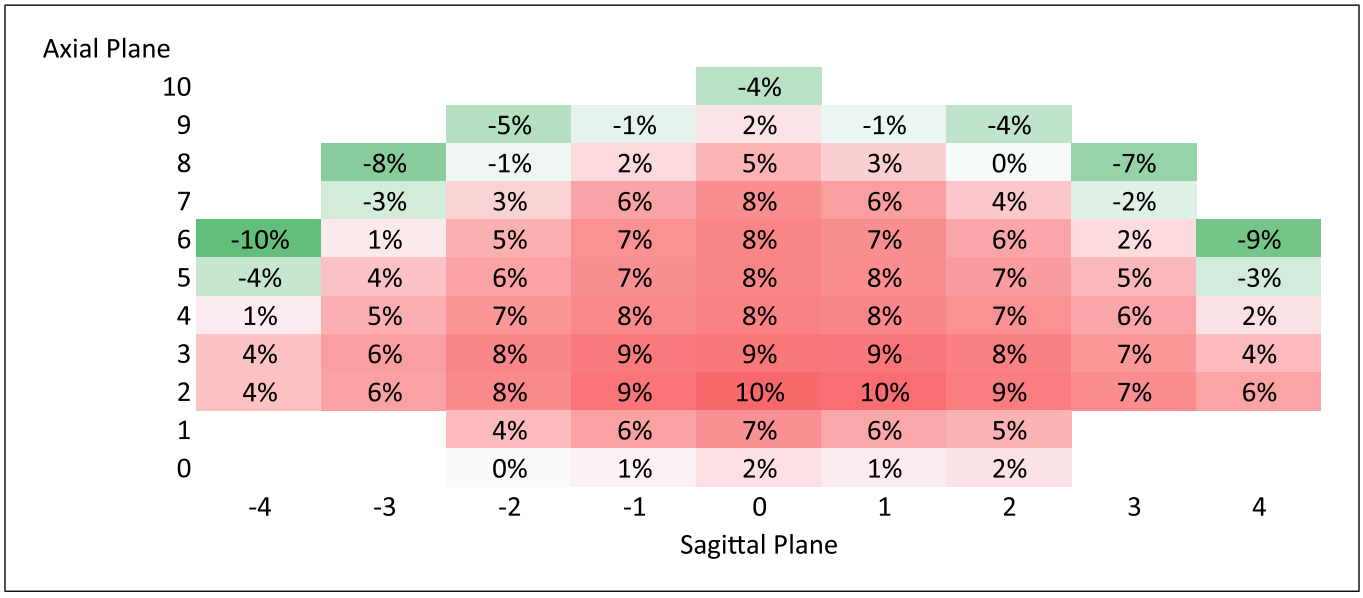

Fig. 3. Population differences between sagittal craniosynostosis and control populations percent difference for each of the posterior (AS) vertices between the SC and control populations. Values are based upon population averages (A) and were calculated as the difference between both populations, divided by the control population ([ASC-AC]/AC) for each posterior point. Only points of intersection that occurred in >90% of individuals were analyzed. Trend indicates that posterior differences in projection increase at more central points.

The classic calvarial shape resulting from SC is generally regarded as an oblong head. The cephalic index, however, is unable to distinguish differences in relative projection anteriorly and posteriorly. A step to evaluate posterior projection was made by Meulstee et al. [24], using a principal component analysis to aid in diagnosis. One such component was the amount of AP length due to occipital elongation. However, this component was used

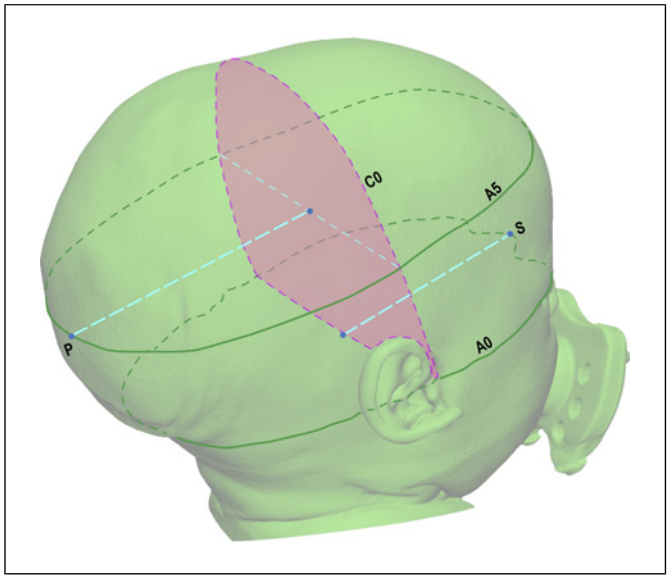

Fig. 4. Occipital bullet index measurement projection of a point (P) was measured as change in the z-axis relative to the mid-coronal plane (C0) at the same axial and sagittal level (zx – 0 or zx). The ratio used to describe the projection of a point for each individual is taken relative to the projection of the sellion (S) to control for head size. Depicted is this measure being taken at the surface intersection of sagittal plane 0 and axial plane 5, the point measured for the OBI.

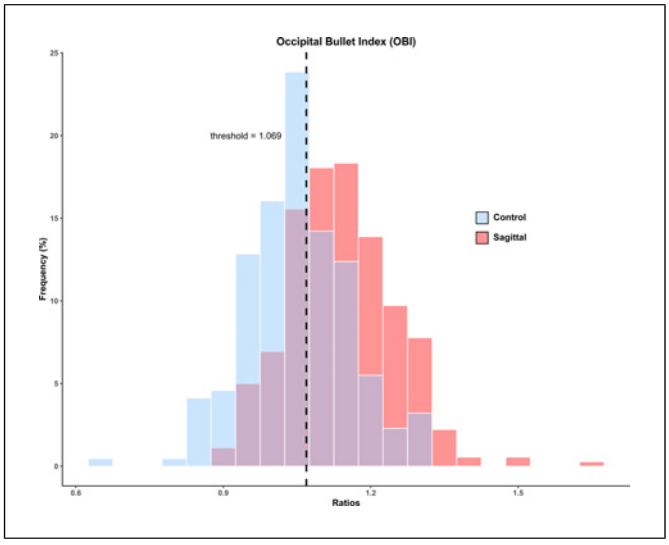

Fig. 5. Performance of the occipital bullet index. By analyzing the projection of point (S0, A5) relative to the sellion, an OBI is created with a maximum sensitivity of 74% and a specificity of 61% at a cutoff of 1.069. The population average is 1.14 for the SC population and 1.05 in the control population, meaning the point has a projection that is typically 14% greater than that of the sellion-origin length in SC and 5% greater in normal individuals.

in conjunction with three others to determine SC diagnosis. This did not create a measure that could be used in isolation but demonstrated feasibility of using posterior projection in conjunction with 3D photography for regional cranial shape analysis.

Historically, the measure perhaps best suited to quantify occipital morphology was the occipital incline angle [2]. This measure evaluates occipital prominence using an angle formed by the intersection between the Frankfort horizontal plane and a line connecting the opisthocranion and inion. This provided a valuable measure of relative protrusion using an internal control based upon CT. However, the measure becomes difficult to replicate using surface anatomy. We found frequent soft tissue interferences at axial levels A0–A2 due to parental hand positioning or excessive posterior neck adiposity on 3D photography in infants, limiting assessment of the lower posterior calvarial surface anatomy.

Ratio-based measures such as the cephalic index allow for comparison between individuals of different head sizes. However, the components of the ratio derive its meaning. For instance, using the cephalic index one cannot evaluate width restriction or compensatory elongation independently but rather the combined relationship between the two. To study a single abnormality, a ratio must be made up of one component that is abnormal and a second that is not. Previously, we created a frontal bossing index (FBI) [16]. The FBI is the ratio of the protrusion of paired superolateral vertices (S ± 3, A5), divided by the protrusion of the sellion (anterior S0, A0). The sellion was selected as the denominator based upon previous studies finding no significant differences in the sella-nasion distance [25] or length of the anterior cranial fossa (n = 20) [26] in patients with SC relative to controls. Here, we attempted to verify that the sellion's protrusion was unaffected by diagnosis. To do this, regression analysis was used to evaluate the effects of age, sex, and diagnosis on head length, width, height, circumference, and sellion protrusion. We found that all measured factors had a statistically significant difference between the two population; given the large sample sizes, our study is powered to detect small degrees of difference. The factors least affected by SC diagnosis were the sellion protrusion, cranial height, and A7 circumference. Of these only the sellion protrusion allows for avoidance of alteration by surgical intervention, allowing for easier interpretation of postoperative changes in the index. We previously utilized sellion projection to determine the FBI and again selected this denominator for normalizing for head size.

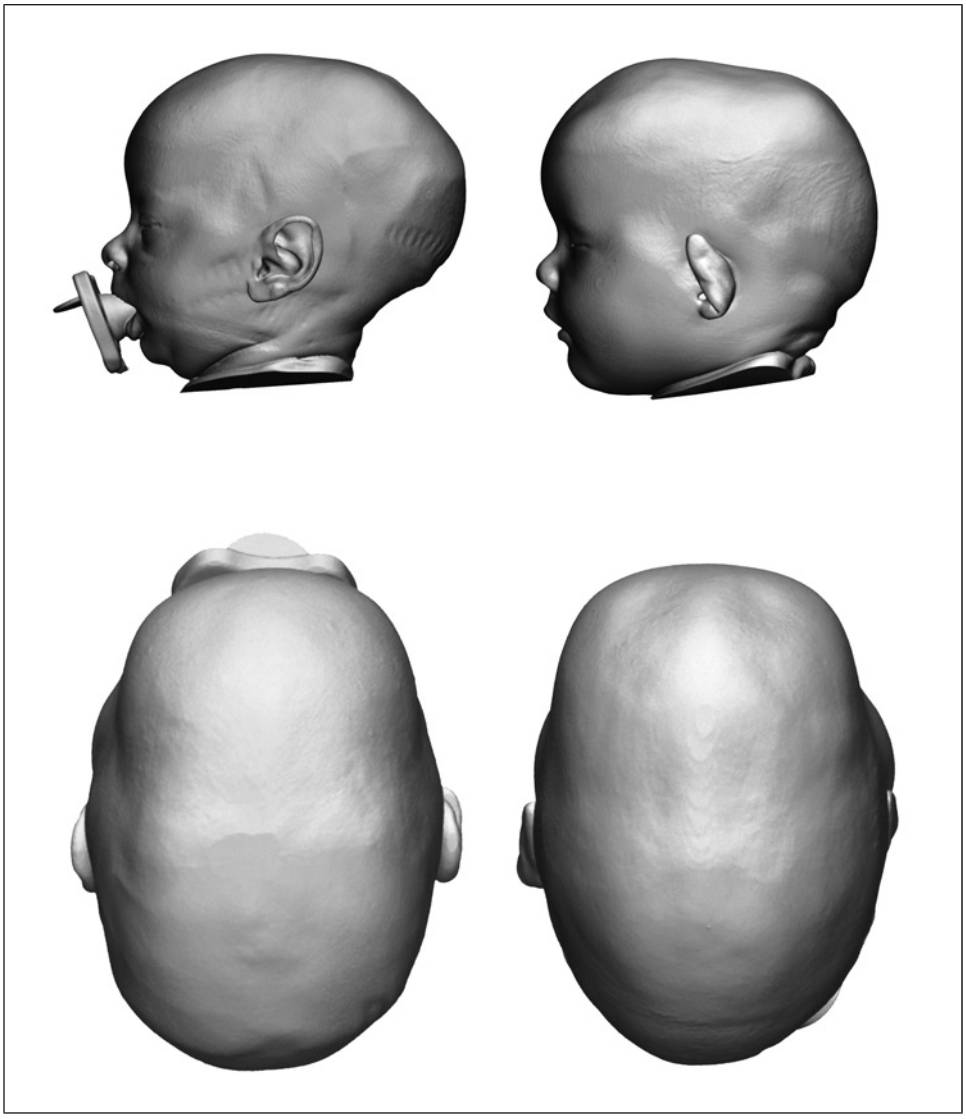

Fig. 6. Clinical application of regional measures. Two individuals (lateral and vertex views) with identical cephalic indexes (71.2) indicating minor scaphocephaly. The patient on the left has an FBI in the 89th percentile and OBI in the 16th, and the patient on the right has an FBI in the 10th percentile and OBI in the 97th. The figure also highlights variable neck adiposity which makes lower axial levels inconsistent in representing surface morphology.

The FBI demonstrated a high sensitivity (93.5%) and specificity (92.9%) for distinguishing control patients from those with SC. In contrast, the OBI has relatively lower diagnostic performance. This is likely due to both a lower magnitude of protrusive difference observed posteriorly (8–10%) compared to frontal bossing (17%) as well as the complex anatomy of the occipital region. The frontal bossing phenotype observed in SC is facilitated in part by the patency of the coronal sutures; the brain is permitted to decompress perpendicular to those sutures. Relative to the coronal sutures the lambdoid sutures have a more oblique orientation, and in the setting of SC posterior compensation allowed by these sutures has both a vertical and horizontal component. The posterior phenotype in SC is variable and may involve different combinations of occipital prominence, vertex narrowing and restriction in posterior vertical height. By limiting analysis of the posterior shape to the OBI in this study, we concede that further work describing vertex narrowing and posterior vertical height will be necessary to gain a complete representation of the SC dysmorphology.

While the OBI alone is predicted to identify infants with a relatively low sensitivity and specificity, when the OBI and FBI are used in tandem to evaluate an individual's length abnormality, sensitivity (94.7%) and specificity (93.1%) are greater than that of the CI (sen = 90%, spec = 92.8%) [27]. This diagnostic ability occurs despite lacking a component measuring biparietal width restriction. A measure that takes the average of both halves as the cephalic index "dilutes" the values of the

more significant prominence and lessens the sensitivity of the test. By looking at both halves as individual measures, the sensitivity/specificity increases. Inclusion of a width component would likely further improve the measure's performance and is the topic of further study.

The inability of the CI to distinguish heads with varying degrees of anterior and posterior prominence but similar total AP length is especially relevant in patients with SC (Fig. 6). Rarely does a preoperative patient have equal degrees of anterior and posterior projection; we found no correlation between the regional severity of the anterior (FBI) and posterior (OBI) prominence in SC (correlation coefficient of 0.019). An elevated OBI relative to the FBI may guide surgeons to focus on the posterior rather than anterior calvarium. Postoperatively, quantifying change that occurs in either hemisphere is important for understanding how an intervention changes head shape and for tracking patient progression over time.

Early attempts have been made to measure the morphology of the calvarium using machine learning [13, 14, 28]. This typically utilizes three-dimensional analysis measuring vectors originating from a central point radiating to the skull surface [13, 14]. These measures are then compared to a simulated skull created using multiple normal individuals allowing for visualization of differences in morphology; however, no metric has been created to describe any aspect of specific regional morphology, as outcomes are primarily qualitative and based on visual interpretation of color. While this model creates a detailed analysis of the exact morphology of the cranium, often visualized as a heat map, it does not yield numeric metric(s) describing severity and regional dysmorphology. While this aids in a surgeon's understanding of a patient's morphology, the models are rarely quantified to allow for scoring, which would aid in provider-patient and provider-provider discussion.

When we assessed senior surgeons' clinical evaluation of the occipital bullet, the degree of correlation between surgeons was found to be greater (ICC = 0.789) than of previous study (ICC = 0.39) [19]. Initial analysis of the metric's CC to clinical evaluation (ICC = 0.568) is between the two indicating adequate clinical correlation. A larger sample of experts across differing institutions is warranted to further validate the tool's correlation with clinical evaluation as our correlation is based on only two clinician's evaluation of bulleting. The increased agreement between surgeon's clinical assessment is potentially due to fewer senior surgeons in this study than previous study (2 vs. 6) [19]. More data from a greater number of surgeons may be helpful to validate and assess the metric's correlation with clinical assessment.

Conclusion

The OBI is a simple tool that surgeons can use to evaluate the regional severity of the posterior morphology of patients with SC. It further has the potential to allow for comparisons in surgical approaches for SC and evaluate changes in cranial morphology over time without the need for radiation. Combined with the FBI these tools allow for more complete understanding of the variable regional dysmorphology associated with SC.

Acknowledgments

We extend our appreciation to Caleb Suggs, Clinical Studies Coordinator, Renea Jenning, Clinical Studies RN, and Margaret Folwell, our Medical Science Photographer, for their indispensable contributions to this research.

Statement of Ethics

Approval was obtained from the Ethics Committee of the Wake Forest School of Medicine. The IRB reference number is IRB00055871. The procedures used in this study adhere to the tenets of the Declaration of Helsinki.

All participants in this study provided written informed consent prior to accessing their CT scans or identifying personal characteristics in this study. This study was also approved by the IRB at Atrium Health Wake Forest Baptist before any data collection commenced. Patients signed informed consent regarding publishing their data and photographs.

Conflict of Interest Statement

The authors have no competing interests to declare that are relevant to the content of this article. None of the authors has a financial interest in any of the products, devices, or drugs mentioned in this manuscript.

Funding Sources

No funding was received to assist with the preparation of this manuscript.

Author Contributions

Authors G.B. and D.C. created head scan models for analysis. Authors G.B., D.C., and R.L. created potential indices. G.B. and B.D. rescored models to determine inter-rater reliability and imaging modality reliability. C.M.R. and L.R.D. scored 3D models for clinical assessments. R.L. completed all statistical analyses. L.Z. created programming capable of automating the OBI. G.B., R.L., S.K., L.R.D., and C.M.R. assisted in manuscript writing. G.B., R.L., S.K., and B.D. collaborated to create figures with exceptional assistance from acknowledged contributor M.F. All authors reviewed the manuscript.

Data Availability Statement

Data are not publicly available due to ethical reasons. Further inquiries can be directed to the corresponding author.

References

1 Janis J. Essentials of plastic Surgery. Essentials Plast Surg. 2014 Mar 5.
2 Seruya M, Tran J, Kumar S, Forrest CR, Chong DK. Computed tomography-based morphometric analysis of extended strip craniectomy for sagittal synostosis. J Craniofac Surg. 2014; 25:42–7.
3 ter Maaten NS, Mazzaferro DM, Wes AM, Naran S, Bartlett SP, Taylor JA. Craniometric analysis of frontal cranial morphology following posterior vault distraction. J Craniofac Surg. 2018;29(5):1169–73.
4 Yen DW, Nguyen DC, Skolnick GB, Naidoo S, Smyth MD, Patel KB, et al. Evaluation of direct surgical remodeling of frontal bossing in patients with sagittal synostosis. J Craniofac Surg. 2019;30(8):2350, 4.
5 Khechoyan D, Schook C, Birgfeld CB, Khosla RK, Saltzman B, Teng CC, et al. Changes in frontal morphology after single-stage open posterior-middle vault expansion for sagittal craniosynostosis. Plast Reconstr Surg. 2012 Feb;129(2):504–16.
6 Le MB, Patel K, Skolnick G, Naidoo S, Smyth M, Kane A, et al. Assessing long-term outcomes of open and endoscopic sagittal synostosis reconstruction using three-dimensional photography. J Craniofac Surg. 2014;25(2):573–576.
7 Raposo-Amaral CE, Denadai R, Takata JPI, Ghizoni E, Buzzo CL, Raposo-Amaral CA. Progressive frontal morphology changes during the first year of a modified Pi procedure for scaphocephaly. Childs Nerv Syst. 2016 Feb;32(2):337–44.
8 David L, Glazier S, Pyle J, Thompson J, Argenta L. Classification system for sagittal craniosynostosis. J Craniofac Surg. 2009; 20(2):279–82.
9 Diab J, Flapper W, Grave B, Abou-Hamden A, Anderson P, Moore M. The Many faces of sagittal synostosis: a novel classification and approach to diagnosis. J Craniofac Surg. 2022 Jan-Feb 01;33(1):192–7.
10 Vu GH, Mazzaferro DM, Kalmar CL, Zimmerman CE, Humphries LS, Swanson JW, et al. Craniometric and volumetric analyses of cranial base and cranial vault differences in patients with nonsyndromic single-suture sagittal craniosynostosis. J Craniofac Surg. 2020 Jun;31(4):1010–14.
11 Calandrelli R, Pilato F, Massimi L, Panfili M, Colosimo C. A systematic quantitative morpho-volumetric analysis in infants with sagittal craniosynostosis and relationship with the severity of scaphocephalic deformity. Radiol Med. 2020 Jun;125(6):585–94.
12 Liaw WXZ, Parr WCH, Peltz TS, Varey A, Hunt J, Gianoutsos M, et al. Quantification of head shape and cranioplasty outcomes: six-compartment volume method applied to sagittal synostosis. Plast Reconstr Surg Glob Open. 2019 Apr 2;7(4):e2171.
13 Marcus JR, Domeshek LF, Das R, Marshall S, Nightingale R, Stokes TH, et al. Objective three-dimensional analysis of cranial morphology. Eplasty. 2008 Apr 9;8:e20.
14 Mendoza CS, Safdar N, Okada K, Myers E, Rogers GF, Linguraru MG. Personalized assessment of craniosynostosis via statistical shape modeling. Med Image Anal. 2014 May 1;18(4):635–46.
15 Lloyd MS, Buchanan EP, Khechoyan DY. Review of quantitative outcome analysis of cranial morphology in craniosynostosis. J Plast Reconstr Aesthet Surg. 2016 Nov 1; 69(11):1464–8.
16 Bins GP, Cull D, Layton R, Powell R, Nearine J, Meegalla N, et al. Measure of frontal morphology in sagittal craniosynostosis: the frontal bossing index. [Under Review].
17 Lepard J, Akbari SHA, Mooney J, Arynchyna A, Iii SGM, Myers RP, et al. Comparison of aesthetic outcomes between open and endoscopically treated sagittal craniosynostosis. J Neurosurg Pediatr. 2021;28(4):432–8.
18 Mooney J, Lepard J, Akbari SHA, Arynchyna A, Myers RP, Grant J, et al. Objective craniometric versus subjective outcome ratings in endoscopic and open sagittal synostosis Surgery. J Craniofac Surg. 2021 May 1;32(3):1090–3.
19 Bendon CL, Johnson HP, Judge AD, Wall SA, Johnson D. The aesthetic outcome of surgical correction for sagittal synostosis can be reliably scored by a novel method of preoperative and postoperative visual assessment. Plast Reconstr Surg. 2014;134(5):775e–86e.
20 You L, Zhang G, Zhao W, Greives M, David L, Zhou X, et al. Automated sagittal craniosynostosis classification from CT images using transfer learning. Clin Surg. 2020 Feb;5.
21 Schmelzer RE, Perlyn CA, Kane AA, Pilgram TK, Govier D, Marsh JL. Identifying reproducible patterns of calvarial dysmorphology in nonsyndromic sagittal craniosynostosis may affect operative intervention and outcomes assessment. Plast Reconstr Surg. 2007 Apr;119(5):1546–52.
22 Druian BR. 10th edVol. 2. In: Sprague R, editor. Northwest anthropological research notes [internet]. Northwest Anthropology. Northwest Anthropology; 1975. [cited 2022 Jun 19]. 175 p. Available from: https://books.google.com/books/about/Northwest_Anthropological_Research_Notes.html?id=0XiDwAAQBAJ.
23 Marcus JR, Stokes TH, Mukundan S, Forrest CR. Quantitative and qualitative assessment of morphology in sagittal synostosis: midsagittal vector analysis. J Craniofac Surg. 2006 Jul;17(4):680–6.
24 Meulstee JW, Verhamme LM, Borstlap WA, van der Heijden F, de Jong GA, Xi T, et al. A new method for three-dimensional evaluation of the cranial shape and the automatic identification of craniosynostosis using 3D stereophotogrammetry. Int J Oral Maxillofac Surg. 2017 Jul 1;46(7):819–26.
25 Guimarães-Ferreira J, Gewalli F, David L, Darvann TA, Hermann NV., Kreiborg S, et al. Sagittal synostosis: I. Preoperative morphology of the skull. Scand J Plast Reconstr Surg Hand Surg. 2006;40(4):193–9.
26 Slomic AM, Bernier JP, Morissette J, Renier D. A craniometric study of sagittal craniosynostosis (SC). J Craniofac Genet Dev Biol. 1992 Jan 1;12:49–54.
27 Ruiz-Correa S, Sze RW, Starr JR, Lin HTJ, Speltz ML, Cunningham ML, et al. New scaphocephaly severity indices of sagittal craniosynostosis: a comparative study with cranial index quantifications. Cleft Palate Craniofac J. 2006 Mar 15;43(2):211–21. https://journals.sagepub.com/doi/abs/10.1597/04-208.1.
28 Tu L, Porras AR, Oh A, Lepore N, Mastromanolis M, Tsering D, et al. Radiation-free quantification of head malformations in craniosynostosis patients from 3D photography. Proc SPIE Int Soc Opt Eng. 2018 Feb; 10575:105751U.